J Supercond Nov Magn (2014) 27:1787–1794
DOI 10.1007/s10948-014-2515-2

ORIGINAL PAPER

Field Dependence of Magnetocaloric Properties in $La_{0.6}Pr_{0.4}Fe_{10.7}Co_{0.8}Si_{1.5}$

R. M'nassri

Received: 28 January 2014 / Accepted: 7 February 2014 / Published online: 11 March 2014

Abstract In this paper, the field dependence of magnetocaloric properties of $La_{0.6}Pr_{0.4}Fe_{10.7}Co_{0.8}Si_{1.5}$ with second-order phase transition material is studied using a phenomenological model. The model parameters were determined from the magnetization data adjustment and were used to give better fits to magnetic transition and to calculate the magnetocaloric thermodynamic quantities. The entropy curves have been observed to behave as an asymmetrical broadening of ΔS_M peak with increasing magnetic field. For larger fields, the peak shifts to higher temperatures, while the overall shape of the curve broadens over a wide temperature range. The values of maximum magnetic entropy change, full width at half maximum, and relative cooling power, at several magnetic field variations, were calculated. The maximum magnetic entropy changes of 3.957(5) and 14.197(4) J kg^{-1} K^{-1} and the relative cooling power (RCP) values of 95.420(3) and 392.729(2) J kg^{-1} are obtained for 1 and 5 T, respectively. The theoretical calculations are compared with the available experimental data. The critical exponents associated with ferromagnetic transition have been determined from magnetocaloric effect (MCE) methods. By using the field dependence of $\Delta S_{M\,max} \approx a(\mu_0 H)^n$ and the distance $(T_{peak} - T_c) \approx b(\mu_0 H)^{1/\Delta}$, we have investigated the critical behavior of $La_{0.6}Pr_{0.4}Fe_{10.7}Co_{0.8}Si_{1.5}$. From the analysis of the relationship between the local exponent n and the gap exponent Δ, we have calculated other exponents: β, γ, and δ. The large MCE, relatively high RCP, high magnetization, and low cost jointly make the present compound a promising candidate for magnetic refrigerant near room temperature.

Keywords Model · Magnetization · Magnetocaloric effect · Critical exponent

R. M'nassri (✉)
Higher Institute of Applied Sciences and Technology of Kasserine, Kairouan University, BP 471, 1200 Kasserine, Tunisia
e-mail: rafik_mnassri@yahoo.fr

1 Introduction

Magnetic materials with large magnetocaloric effect (MCE) have been extensively studied experimentally and theoretically due to their great potential applications in energy-efficient magnetic refrigeration (MR) technology [1–3]. The reason for this is twofold. On the one hand, magnetic cooling offers a competitive alternative to conventional gas compression–expansion refrigeration systems due to its high energy efficiency and environmental friendliness, as neither ozone-depleting nor global warming volatile refrigerants are required. On the other hand, as magnetic refrigeration close to room temperature is only possible with materials which undergo a phase transition close to the working temperature of a refrigerator, the characterization of magnetocaloric materials generally tends to become associated with a detailed study of their phase transition, which is also interesting from a fundamental point of view. Numerous magnetocaloric materials have been intensively studied these years because of their possibility for applications in magnetic refrigeration near room temperature region, e.g., $Gd_5Si_2Ge_2$ alloy [4], NiMnGa [5, 6], $FeMnP_{1-x}As_x$ [7], $LaFe_{13-x}Si_x$ [8], and ferromagnetic perovskite

maganites [9–13]. With prominent advantages in terms of giant magnetic entropy change ΔS_M, $LaFe_{13-x}Si_x$ has been the progenitor of recent focused efforts regarding the magnetocaloric effect in a variety of systems because it uses relatively common, low-toxicity elements; low-cost, excellent soft ferromagnetism; and high magnetization, and it has a large magnetocaloric effect [8]. For $LaFe_{13-x}Si_x$, the phase transition is very sensitive to the Si content, i.e., it changes from first-order transition to second-order transition corresponding to the Si content from $1.0 \leq x \leq 1.6$ to $1.6 < x \leq 2.0$, respectively. The Si element was introduced to stabilize a cubic NaZn13-type structure. The Curie temperature (T_C) in the base LaFeSi material occurs more than 70 K below room temperature, but magnetic transition can be raised to room temperature or above by the addition of H as an interstitial element or substitution of Co for Fe [14]. To obtain a large ΔS_M material without a thermal and magnetic hysteresis which is workable in a wide range of temperatures near room temperature [15], we have studied the effect of combined substitution of Pr and Co on the MCE of NaZn13-type $La_{0.6}Pr_{0.4}Fe_{10.7}Co_{0.8}Si_{1.5}$ compound. The praseodymium was introduced as the substitute element to increase the magnetic entropy change. In this work, we investigated the magnetocaloric properties for the optimized $La_{0.6}Pr_{0.4}Fe_{10.7}Co_{0.8}Si_{1.5}$ compound. The sample was prepared by arc melting in a high-purity argon atmosphere. $La_{0.6}Pr_{0.4}Fe_{10.7}Co_{0.8}Si_{1.5}$ was turned over and remelted several times to make certain its homogeneity. The obtained ingot was wrapped using a molybdenum foil, sealed in a high-vacuum quartz tube, annealed at 1,373 K for 40 days, and then quenched into liquid nitrogen [16].

2 Model Calculations

According to the phenomenological model [17], the dependence of magnetization on a variation of temperature and Curie temperature T_C is presented by

$$M(T, H = H_{max}) = \left(\frac{M_i - M_f}{2}\right)[\tanh(A(T_C - T))] + BT + C \tag{1}$$

where H_{max} is the maximum external field, T_C is the Curie temperature, and M_i/M_f is the initial/final value of magnetization at ferromagnetic–paramagnetic transition as shown in Fig. 1. Here, $A = 2\left(\frac{B-S_c}{M_i-M_f}\right)$, B is the magnetization sensitivity dM/dT at ferromagnetic state before transition, S_c is the magnetization sensitivity dM/dT at Curie temperature T_C, and $C = \left(\frac{M_i-M_f}{2}\right) - BT_C$

The magnetic entropy change (ΔS_M) can be obtained through the adiabatic change of temperature by the application of a magnetic field. ΔS_M as a function of temperature for a field variation from 0 to H_{max} is given by

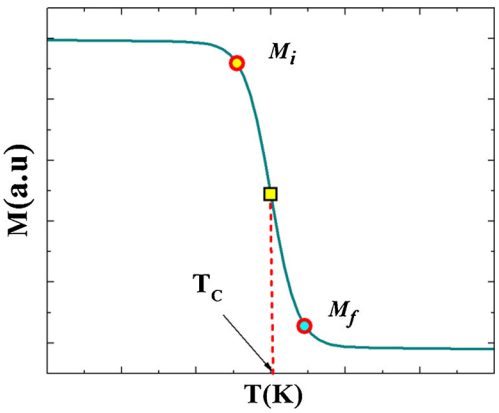

Fig. 1 Temperature dependence of magnetization in constantly applied magnetic field

$$\Delta S_M(T, \Delta H = H_{max}) = H_{max}\left[-A\left(\frac{M_i - M_f}{2}\right)\mathrm{sech}^2(A(T_C - T)) + B\right] \tag{2}$$

A more abrupt variation of magnetization near the magnetic transition occurs and results in a large magnetic entropy change. ΔS_M depends on the temperature gradient of magnetization and reaches a maximum value around T_C.

Relative cooling power (RCP) is a useful parameter which decides the efficiency of magnetocaloric materials based on the magnetic entropy change [1, 18]. The RCP is defined as the product of maximum magnetic entropy change ΔS_{Mmax} and full width at half maximum in $\Delta S_M(T)$ curve (δT_{FWHM}). According to this model, ΔS_{Mmax} is available by

$$\Delta S_{Mmax} = H_{max}\left[-A\left(\frac{M_i - M_f}{2}\right) + B\right] \tag{3}$$

and δT_{FWHM} is presented by

$$\delta T_{FWHM} = \frac{2}{A}\cosh^{-1}\left(\frac{2A(M_i - M_f)}{A(M_i - M_f) + 2B}\right)^{1/2} \tag{4}$$

Then, RCP is computed by

$$\begin{aligned} RCP &= -\Delta S_{Mmax}\delta T_{FWHM} \\ &= H_{max}\left(M_i - M_f - \frac{2B}{A}\right)\cosh^{-1}\left(\frac{2A(M_i - M_f)}{A(M_i - M_f) + 2B}\right)^{1/2} \end{aligned} \tag{5}$$

The RCP corresponds to the amount of heat that can be transferred between the cold and hot parts of a refrigerator in one ideal thermodynamic cycle. This parameter allows an easy comparison of different magnetic materials for applications in magnetic refrigeration; hence, larger RCP values lead to better magnetocaloric materials.

Table 1 Model parameters for $La_{0.6}Pr_{0.4}Fe_{10.7}Co_{0.8}Si_{1.5}$ system at several magnetic fields

$\mu_0 H(T)$	T_C (K)	M_i (emu/g)	M_f (emu/g)	B (emu/g/K)	S_c (emu/g/K)
0.5	269	118.208	5.1555	−0.01	−4.0406
1	270.5	113.73064	19.98244	−0.3	−3.95756
2	271	111.72959	33.02312	−0.45	−3.70849
3	273	114.129	35.25022	−0.4	−3.35793
4	274	114.129	42.9475	−0.45	−3.04427
5	275	112.52561	48.91425	−0.47	−2.83948

Another figure of merit which is used to compare the magnetic refrigerant materials is the refrigerant capacity (RC). The RC can be determinate by numerically integrating the area under the $\Delta S_M(T)$ curve using the temperatures at half maximum of the peak as integration limits [19]. Here, RC value can be obtained as

$$\begin{aligned} RC &= -\int_{T_C+\frac{\delta T_{FWHM}}{2}}^{T_C-\frac{\delta T_{FWHM}}{2}} \Delta S(T)dT \\ &= H_{max}\left[-(M_i-M_f)\tanh\left(A\frac{\delta T_{FWHM}}{2}\right)+B\delta T_{FWHM}\right] \end{aligned} \quad (6)$$

The heat capacity can be calculated from the magnetic contribution to the entropy change induced in the material, $\Delta C_{P,H}$, by the following expression:

$$\Delta C_{P,H} = T\frac{\partial \Delta S_M}{\partial T} \quad (7)$$

From this model, a determination of $\Delta C_{P,H}$ can be carried out as follows:

$$\begin{aligned} &\Delta C_{P,H}(T, \Delta H = H_{max}) \\ &= H_{max}[-TA^2(M_i-M_f)\mathrm{sech}^2(A(T_C-T))\tanh(A(T_C-T))] \end{aligned} \quad (8)$$

From this phenomenological model, it can easily assess the values of δT_{FWHM}, ΔS_{Mmax}, RCP, RC, and $\Delta C_{P,Hmin/max}$ for $La_{0.6}Pr_{0.4}Fe_{10.7}Co_{0.8}Si_{1.5}$ at several magnetic fields.

3 Model Application and Discussions

In order to apply phenomenological model, numerical calculations were made with parameters as displayed in Table 1. Figure 2 depicts the magnetization versus temperature in different applied magnetic field shifts for $La_{0.6}Pr_{0.4}Fe_{10.7}Co_{0.8}Si_{1.5}$ that has been prepared by arc melting in a high-purity argon atmosphere. The symbols represent experimental data from [16], while the dashed

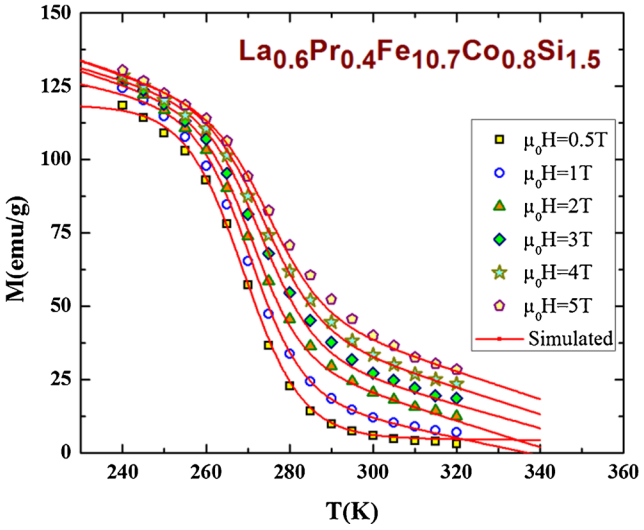

Fig. 2 Magnetization versus temperature for the $La_{0.6}Pr_{0.4}Fe_{10.7}Co_{0.8}Si_{1.5}$ system at several magnetic fields. The *solid lines* are modeled results, and *symbols* represent experimental data from [16]

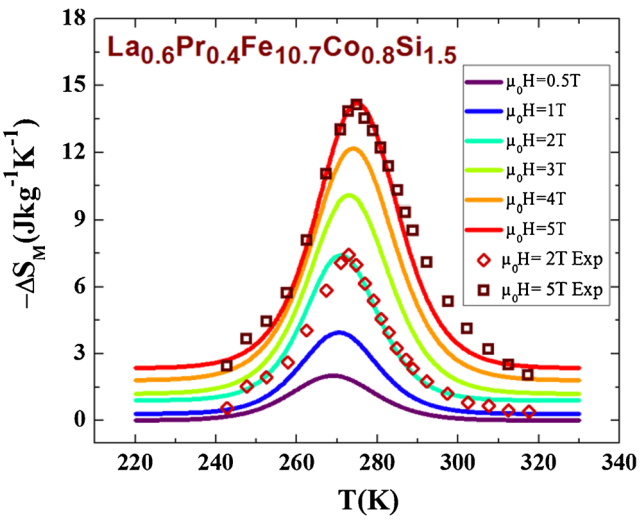

Fig. 3 Magnetic entropy change, ΔS, for the $La_{0.6}Pr_{0.4}Fe_{10.7}Co_{0.8}Si_{1.5}$ sample. The *solid lines* are predicted results, and *symbols* represent experimental data from [16]

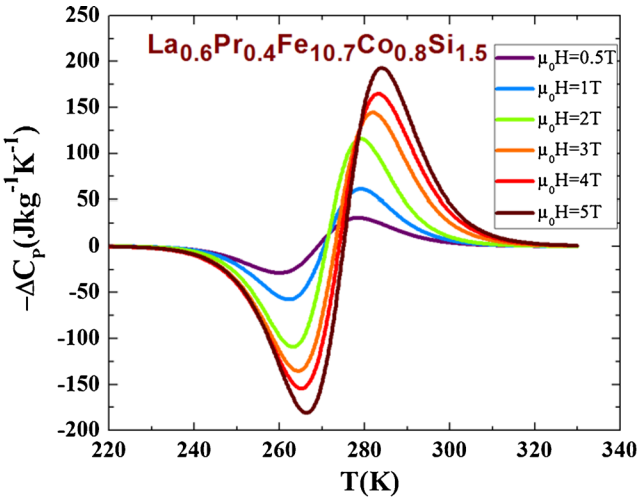

Fig. 4 Heat capacity change for ΔC_P for $La_{0.6}Pr_{0.4}Fe_{10.7}Co_{0.8}Si_{1.5}$ system

curves represent modeled data using model parameters given in Table 1. It is seen that for the given parameters, the results of calculation are in a good agreement with the experimental results. Magnetic transition in $La_{0.6}Pr_{0.4}Fe_{10.7}Co_{0.8}Si_{1.5}$ is reversible in a cycle of increasing and decreasing temperature, being accompanied without any thermal hysteresis which is highly desired in the sense of practical application. It can be reported that the magnetization exhibits a continuous change around T_C in different magnetic fields, and T_C significantly increases with the increase in magnetic field [16].

Furthermore, Figs. 3 and 4 show predicted values for changes of magnetic entropy and specific heat. Magnetic entropy change in $La_{0.6}Pr_{0.4}Fe_{10.7}Co_{0.8}Si_{1.5}$ is reported for $\Delta H = 0.5$, 1, 2, 3, 4, and 5 T in Fig. 3 and show an increase in $-\Delta S_M$ with increasing ΔH. The $-\Delta S_M$ is found to be positive in the entire temperature range for all magnetic fields that confirmed the ferromagnetic character. It is seen that the results of calculation are in a good agreement with the experimental results. The magnetocaloric effect increases with an increase of the applied magnetic field and with the change of magnetization during the application of magnetic field. This means that the effect reaches its maximum in the vicinity of magnetic phase transition points. The large values of ΔS_M for $La_{0.6}Pr_{0.4}Fe_{10.7}Co_{0.8}Si_{1.5}$ compounds originate from a reversible second-order magnetic transition [16]. For $\Delta H = 0.5$ T, the ΔS_M shows a maximum value of 2.020(3) J kg^{-1} K^{-1} around 269 K, and it decreases symmetrically on either side. The magnitude of ΔS_M increases with an increasing strength of H and reaches a maximum value of 14.197(4) J kg^{-1} K^{-1} for $\Delta H = 5$ T. However, the peak of ΔS_M becomes asymmetrical at higher fields, i.e., while ΔS_M decreases sharply with lowering temperature below the peak, it decreases gradually with an increasing temperature above the peak. Furthermore, the position of peak shifts to higher temperature with an increasing strength of H, i.e., the peak shifts from 269 K for $\Delta H = 0.5$ T to 275 K for $\Delta H = 5$ T.

At the individual temperatures, the field dependence of the isothermal magnetic entropy change of sample $La_{0.6}Pr_{0.4}Fe_{10.7}Co_{0.8}Si_{1.5}$, as deduced from Fig. 3 curves, is consistent with a simple ferromagnetic order (i.e., a monotonic, almost linear increase is seen) over the total investigated field and temperature range. Figure 5a, b, for temperatures below and above the transition, respectively, shows $-\Delta S_M$ changes to a positive value with the increase of the magnetic field, corresponding to the magnetic transition from ferromagnetic to paramagnetic states.

At the peak, the field dependence of $-\Delta S_M$ can be assumed to be a power law, with an exponent n

$$\Delta S_{Mmax} \approx a(\mu_0 H)^n \tag{9}$$

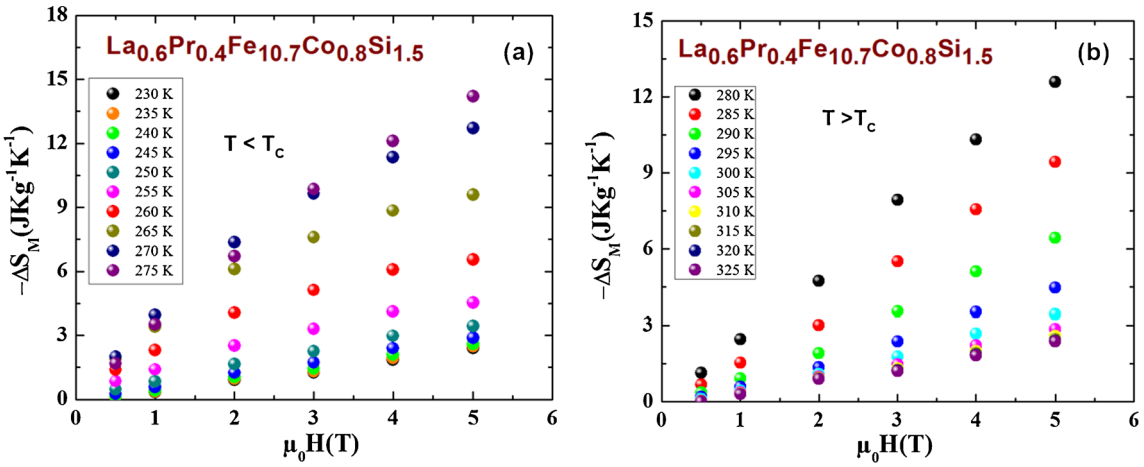

Fig. 5 Isothermal magnetic entropy change versus maximal field applied for $La_{0.6}Pr_{0.4}Fe_{10.7}Co_{0.8}Si_{1.5}$, as selected temperatures below or above transition (**a**, **b**), respectively

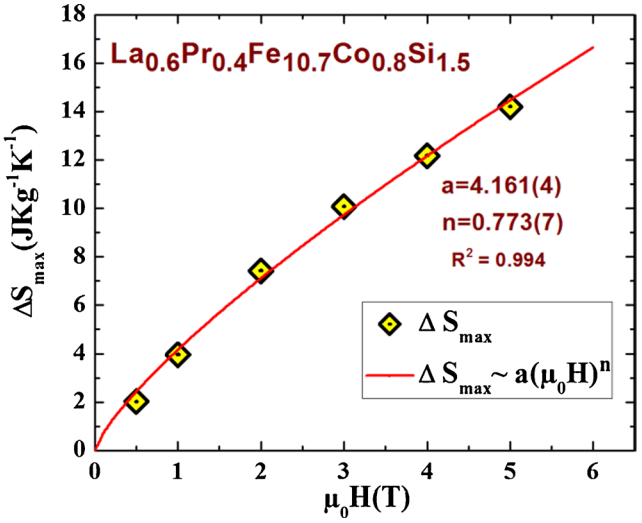

Fig. 6 Field dependence of maximum magnetic entropy change for $La_{0.6}Pr_{0.4}Fe_{10.7}Co_{0.8}Si_{1.5}$

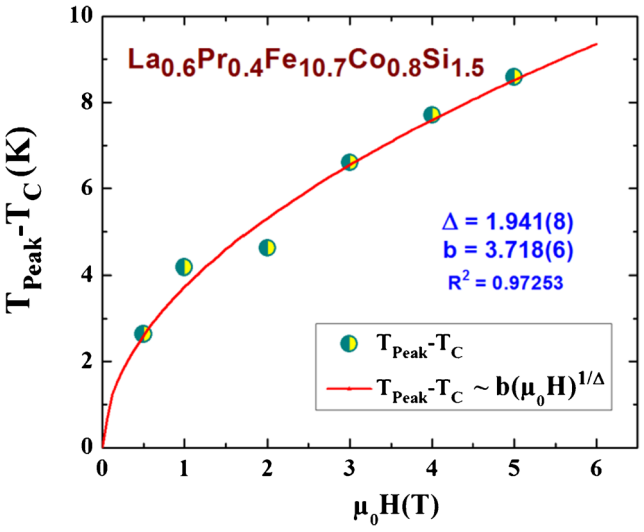

Fig. 8 Field dependence of the distance (T_{peak}–T_C) for $La_{0.6}Pr_{0.4}Fe_{10.7}Co_{0.8}Si_{1.5}$

At T_C, the exponent n becomes field-independent and is expressed as

$$n(T_C) = \left(\frac{\beta - 1}{\beta + \gamma}\right) + 1 \tag{10}$$

where β and γ are the critical exponents [20].

As shown in Fig. 6, the fitting of full square points (ΔS_{Mmax}) leads to that $n(T_C) = 0.773(5)$ for $La_{0.6}Pr_{0.4}Fe_{10.7}Co_{0.8}Si_{1.5}$, which is larger than the predicted value of 2/3 in the mean field approach [21] due to the local inhomogeneities in $La_{0.6}Pr_{0.4}Fe_{10.7}Co_{0.8}Si_{1.5}$.

In addition to the magnitude of the ΔS_M, other important parameters used to characterize the refrigerant efficiency of the material are the RCP and RC defined as Eqs. (5) and (6).

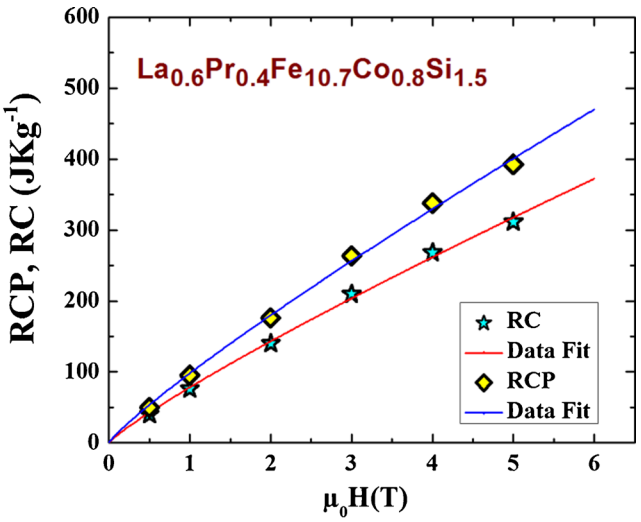

Fig. 7 Field dependence of RCP and RC for $La_{0.6}Pr_{0.4}Fe_{10.7}Co_{0.8}Si_{1.5}$

RCP and RC give an estimate of quantity of the heat transfer between the hot (T_{hot}) and cold (T_{cold}) ends during one refrigeration cycle, and it is the area under the ΔS_M versus T curve between two temperatures ($\Delta T = T_{hot}$–T_{cold}) of the FWHM of the curve. Figure 7 shows the values for the compound $LaFe_{10.7}Co_{0.8}Si_{1.5}$ as a function of applied magnetic field.

The MCE data of different materials of the same universality class should fall onto the same curve irrespective of the applied magnetic field. Because of the intrinsic relation between the MCE and the universality class, one can obtain the critical exponents based on the MCE data, which may be another method to determine the critical behavior of phase transition, i.e., the universality class. Based

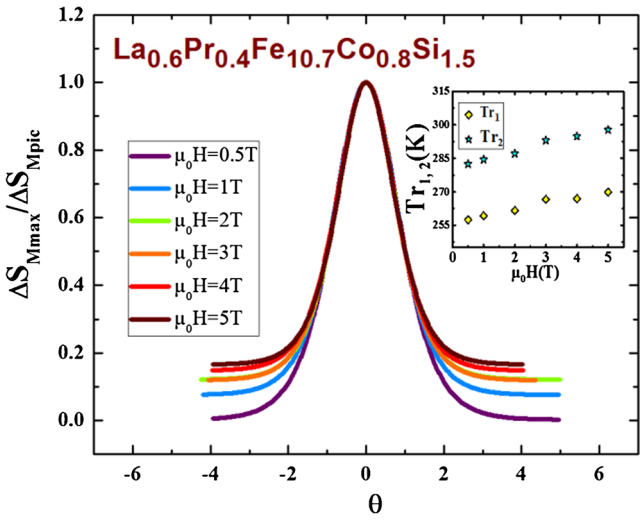

Fig. 9 Normalized entropy change as a function of the rescaled temperature θ. The *inset* shows the magnetic field dependences of the two reference temperatures (T_{r1} and T_{r2})

Table 2 Comparison of maximum entropy change, specific heat change, RCP, and RC for $La_{0.6}Pr_{0.4}Fe_{10.7}Co_{0.8}Si_{1.5}$ system and several materials

Material	μ_0H(T)	ΔS_{max} (J kg^{-1} K^{-1})	δT_{FWHM} (K)	RCP (J kg^{-1})	RC (J kg^{-1})	$\Delta C_{P,Hmin}$ (J kg^{-1} K^{-1})	$\Delta C_{P,Hmax}$ (J kg^{-1} K^{-1})	Ref.
$La_{0.6}Pr_{0.4}Fe_{10.7}Co_{0.8}Si_{1.5}$	0.5	2.020(3)	24.770(4)	50.043(8)	40.143(5)	−28.741(1)	30.784(2)	Present
	1	3.957(5)	24.110(8)	95.420(3)	76.188(3)	−57.583(8)	61.299(5)	Present
	2	7.416(9)	23.743(2)	176.103(2)	140.114(1)	−109.292(6)	115.898(8)	Present
	3	10.073(8)	26.154(2)	263.472(6)	209.667(4)	−135.401(7)	144.405(7)	Present
	4	12.177(1)	27.726(9)	337.633(7)	268.003(6)	−154.323747	164.838(9)	Present
	5	14.197(4)	27.662(1)	392.729(2)	311.202(7)	−180.900(5)	192.900(8)	Present
$La_{0.5}Pr_{0.5}Fe_{10.7}Co_{0.8}Si_{1.5}C_{0.2}$	2	5.8	–	–	–	–	–	Shen and Zhao [35]
	5	11.6	–	–	386	–	–	Shen and Zhao [35]
$La(Fe_{0.98}Co_{0.02})_{11.7}Al_{1.3}$	5	10.6	–	–	–	–	–	Hu et al. [36]
$La(Fe_{0.92}Co_{0.08})_{11.9}Si_{1.1}$	5	15.6	–	–	–	–	–	Hu et al. [37]
$LaFe_{11.2}Co_{0.7}Si_{1.1}$	5	20.3	–	–	–	–	–	Hu et al. [38]
$LaFe_{10.7}Co_{0.8}Si_{1.5}$	0.5	1.99446	26.91034	53.6716	–	−27.2216912	29.2335969	M'nassri and Cheikhrouhou [15]
	1	4.03047	25.59544	103.16165	–	−57.6795499	61.4306228	M'nassri and Cheikhrouhou [15]
	2	7.10526	28.34153	201.37396	–	−92.6188344	99.0138624	M'nassri and Cheikhrouhou [15]
	3	9.63987	29.79584	287.22806	–	−120.336525	128.981128	M'nassri and Cheikhrouhou [15]
	4	11.759	31.25734	367.55507	–	−141.042779	150.949928	M'nassri and Cheikhrouhou [15]
	5	13.5173	32.76171	442.84992	–	−155.090159	166.624692	M'nassri and Cheikhrouhou [15]
$La_{2/3}Ba_{1/3}MnO_3$	1	2.788	25.035	69.809	–	−49.343	51.898	M'nassri and Cheikhrouhou [28]
$La_{2/3}Ba_{1/3}MnO_{2.98}$	1	2.745	23.853	65.492	–	−45.794	49.297	M'nassri and Cheikhrouhou [28]
Dy	6.5	19.50	–	–	–	−100	290	Foldeaki et al. [39]
Gd	1	3.25	–	–	–	−80	37	Foldeaki et al. [39]

on Fig. 8, the field dependence of the distance $T_{peak} - T_C$ for $La_{0.6}Pr_{0.4}Fe_{10.7}Co_{0.8}Si_{1.5}$ is depicted. The distance between T_C and T_{peak} increases with field following a power law $b(\mu_0 H)^{1/\Delta}$ (where b is the constant, and Δ is the gap exponent), as predicted by scaling laws [22]. This feature provides an insight into the critical behavior of the compound. The lowest field data have been omitted because of the large uncertainty of the peak position. The slope of the linear function fitted to the Ln–Ln data yields the inverse of the gap exponent which implies $\Delta = 1.941(8)$.

The knowledge of two critical exponents n and Δ inferred from the field dependence of MCE is enough to determine other exponents, e.g., β and γ [23]. By means of the relation $\Delta = \beta + \gamma$ and Eq. (10), one can effortlessly finds that $\beta = 1 - \Delta(1 - n) \approx 0.560(5)$ and that $\gamma = \Delta(2 - n) - 1 \approx 1.381(2)$. Fundamentally, β keeps close to the value of the mean field universality class associated with long-range FM interactions, while γ is paradoxically close to the value expected for the 3D Heisenberg ferromagnets with ferromagnetic short-range interactions. A similar result of critical behaviors was observed in $Pr_{0.3}Nd_{0.2}Sr_{0.5}MnO_3$ [24]. Together with β and γ, the other exponent δ can be also determined from the Widom's relation [25]: $\delta = 1 + \gamma / \beta \approx 3.463(9)$.

Using Eq. (8), one can calculate the specific heat changes, $\Delta C_{P,H}$, caused by the applied magnetic field. Shown in Fig. 4 is $\Delta C_{P,H}$ as a function of temperature for $\mu_0 H = 0.5$, 1, 2, 3, 4, and 5 T. It is clearly seen that $\Delta C_{P,H}$ changes sharply from negative to positive at the Curie temperature. Since $\partial M / \partial T < 0$, $\Delta S_M < 0$ results, and accordingly, the total entropy decreases upon magnetization. Furthermore, $\Delta C_{P,H} < 0$ for $T < T_C$ and $\Delta C_{P,H} > 0$ for $T > T_C$ [13, 26]. The sum of the two parts is the magnetic contribution to the total specific heat which affects the cooling or heating power of the magnetic refrigerator [27]. Specific heat presents the advantage of delivering values necessary for further refrigerator design, should the material in question be selected.

For comparison, we have also tabulated the thermomagnetic properties for several magnetocaloric materials under different magnetic fields (see Table 2).

Recently, we [28] and others [29, 30] have shown that for second-order magnetic transition materials, the $\Delta S_M(T)$ curves obtained with different maximum applied fields will collapse onto a universal curve by normalizing all the ΔS_M curves with their peak entropy change, respectively, as $\Delta S'_M = \Delta S_M / 2$, and the temperature axis has to be rescaled in a different way below and above T_C, just by imposing that the position of two additional reference points in the curve correspond to new parameter θ, defined by the expression [28, 31]

$$\theta = \begin{cases} -(T - T_C)/(T_{r1} - T_C); & T \le T_C \\ (T - T_C)/(T_{r2} - T_C); & T > T_C \end{cases} \quad (11)$$

where T_{r1} and T_{r2} are the reference temperatures below and above T_C, respectively.

The phenomenological construction of the universal scaling of different magnetic fields is depicted in Fig. 9. Figure 9 shows an attempt to form a master curve for the entropy change of the $La_{0.6}Pr_{0.4}Fe_{10.7}Co_{0.8}Si_{1.5}$. One can see that the universal behavior manifests itself only in a limited interval around the peak temperature. Farther below and above the peak, the scaling behavior apparently breaks. Increasing fields produce an increase in the reduced magnetic entropy change. Deviations from the collapse might indicate either the influence of the demagnetizing field associated to the shape of the sample [32] or the presence of additional magnetic phases [33, 34]. The divergence of the curves is clear in the compound, particularly above the T_C. The inset of Fig. 9 shows the magnetic field dependences of the two reference temperatures (T_{r1} and T_{r2}). Both the temperatures increase with increasing field.

4 Conclusions

In summary, the exhibition of large MCE in $La_{0.6}Pr_{0.4}Fe_{10.7}Co_{0.8}Si_{1.5}$ which is associated with a ferromagnetic to paramagnetic phase transition near the Curie temperature was reported.

Dependence of the magnetization on temperature variation for $La_{0.6}Pr_{0.4}Fe_{10.7}Co_{0.8}Si_{1.5}$ upon different magnetic fields was simulated. A good magnetocaloric property is observed. The large change of magnetization during the phase transition leads to large MCE. Large ΔS_M of 7.416(9) J kg^{-1} K^{-1} and RCP of 176.103(2) J kg^{-1} are found for a magnetic field change of 0–2 T. Large MCE originates from a reversible second-order magnetic transition. The peak of the $\Delta S_{Mmax}(T)$ curve shows a broad distribution, and the full width at half maximum of the ΔS_{Mmax} peak is about 392.729(2) (Table 2) under a magnetic field of 5 T. We show that the higher field $La_{0.6}Pr_{0.4}Fe_{10.7}Co_{0.8}Si_{1.5}$ MCE has a power law field dependence characterized by an exponent $n = 0.773(7)$. The critical exponents associated with ferromagnetic transition have been determined from the magnetocaloric effect (MCE) methods. This sample exhibits considerably no magnetic hysteresis near room temperature, which is beneficial for the magnetic cooling efficiency. Moreover, by virtue of the excellent MCE with the low cost, high safety, easy preparation, and tunable Curie temperature, the $La_{0.6}Pr_{0.4}Fe_{10.7}Co_{0.8}Si_{1.5}$ system appears to be a good candidate for magnetic refrigerant materials at near room temperature range.

Acknowledgments This study was supported by the Tunisian Ministry of Higher Education and Scientific Research.

References

1. Gschneidner, K.A. Jr.., Pecharsky, V.K., Tsokol, A.O.: Rep. Progr. Phys. **68**, 4179 (2005)
2. Gschneidner, K.A. Jr.., Pecharsky, V.K.: Mater. Sci. Eng. A **287**, 301 (2000)
3. Gschneidner, K.A. Jr.., Pecharsky, V.K.: J. Appl. Phys. **85**, 5365 (1999)
4. Pecharsky, V.K., Gschneidner, K.A. Jr.: Phys. Rev. Lett. **78**, 4494 (1997)
5. Hu, F.X., et al.: Phys. Rev. B **132412**, 64 (2001)
6. Hu, F.X., Shen, B.G., Sun, J.R.: Appl. Phys. Lett. **76**, 3460 (2000)
7. Tegus, O., Bruck, E., Buschow, K.H.J., De Boer, F.R.: Nature (London) **415**, 150 (2002)
8. Hu, F.X., Shen, B.G., Sun, J.R., Cheng, Z.H., Rao, G.H., Zhang, X.X.: Appl. Phys. Lett. **78**, 3675 (2001)
9. Phan, M.H., Yu, S.C.: J. Magn. Magn. Mater. **308**, 325 (2007)
10. M'nassri, R., Cheikhrouhou-Koubaa, W., Koubaa, M., Boudjada, N., Cheikhrouhou, A.: Solid State Commun. **151**, 1579 (2011)
11. M'nassri, R., Cheikhrouhou-Koubaa, W., Chniba-Boudjada, N., Cheikhrouhou, A.: J. Appl. Phys. **073905**, 113 (2013)
12. M'nassri, R., Cheikhrouhou-Koubaa, W., Boudjada, N., Cheikhrouhou, A.: J. Supercond. Nov. Magn. **26**, 1429 (2013)
13. M'nassri, R., Cheikhrouhou, A.: J. Supercond. Nov. Magn. **27**, 421 (2014)
14. Hu, F.X., Qian, X.L., Sun, J.R., Wang, G.J., Zhang, X.X., et al.: J. Appl. Phys. **92**, 3620 (2002)
15. M'nassri, R., Cheikhrouhou, A.: J. Supercond. Nov. Magn. doi:10.1007/s10948-013-2375-1
16. Shen, J., Gao, B., Dong, Q.-Y., Li, Y.-X., Hu, F.-X., Sun, J.-R., Shen, B.-G.: J. Phys. D Appl. Phys. **41**, 245005 (2008)
17. Hamad, M.A.: Phase Transitions **85**, 106 (2012)
18. Gschneidner, K.A., Pecharsky, V.K. Jr.: Annu. Rev. Mater. Sci. **30**, 387 (2000)
19. Gschneidner, K.A. Jr.., Pecharsky, V.K., Pecharsky, A.O., Zimm, C.B.: Mater. Sci. Forum. **315**, 69 (1999)
20. Franco, V., Conde, A.: Int. J. Refrig. **33**, 465 (2010)
21. Franco, V., Blazquez, J.S., Conde, A.: Appl. Phys. Lett. **222512**, 89 (2006)
22. Franco, V., Conde, A., Romero-Enrique, J.M., Blázquez, J.S.: J. Phys.: Condens. Matter. **285207**, 20 (2008)
23. Pelka, R., Konieczny, P., Zielinski, P.M., Wasiutynski, T., Miyazaki, Y., Inaba, A., Pinkowicz, D., Sieklucka, B.: J. Magn. Magn. Mater. **354**, 359 (2014)
24. Zhang, P., Thanh, T.D., Phan, T.-L., Yu, S.C.: J. Appl. Phys. **113**, 17E144 (2013)
25. Stanley, H.E.: Introduction to Phase Transitions and Critical Phenomena. Oxford University Press, London (1971)
26. Yang, H., Zhu, Y.H., Xian, T., Jiang, J.L.: J. Alloys Compd. **555**, 150 (2013)
27. Zhang, X.X., Wen, G.H., Wang, F.W., Wang, W.H., Yu, C.H., et al.: Appl. Phys. Lett. **77**, 3072 (2000)
28. M'nassri, R., Cheikhrouhou, A.: J. Supercond. Nov. Magn. doi:10.1007/s10948-013-2459-y
29. Franco, V., Conde, A., Pecharsky, V.K., Gschneidner, K.A. Jr.: Europhys. Lett. **79**, 47009 (2007)
30. Franco, V., Conde, A., Sidhaye, D., Prasad, B.L.V., Poddar, P., Srinath, S., Phan, M.H., Srikanth, H.: J. Appl. Phys. **107**, 09A902 (2010)
31. Franco, V., Blazquez, J.S., Conde, A.: Appl. Phys. Lett. **89**, 222512 (2006)
32. Caballero-Flores, R., Franco, V., Conde, A., Kiss, L.F.: J. Appl. Phys. **105**, 07A919 (2009)
33. Franco, V., Conde, A., Provenzano, V., Shull, R.D.: J. Magn. Magn. Mater. **322**, 218 (2010)
34. Franco, V., Caballero-Flores, R., Conde, A., Dong, Q.Y., Zhang, H.W.: J. Magn. Magn. Mater. **321**, 1115 (2009)
35. Shen, J., Zhao, J.-L.: J. Appl. Phys. **111**, 07A908 (2012)
36. Hu, F.X., Shen, B.G., Sun, J.R., Zhang, X.X.: Chin. Phys. **9**, 550 (2000)
37. Hu, F.X., Gao, J., Qian, X.L., Ilyn, M., Tishin, A.M., Sun, J.R., Shen, B.G.: J. Appl. Phys. **97**, 10M303 (2005)
38. Hu, F.X., Shen, B.G., Sun, J.R., Wang, G.J., Cheng, Z.H.: Appl. Phys. Lett. **80**, 826 (2002)
39. Foldeaki, M., Chahine, R., Bose, T.K.: J. Appl. Phys. **77**, 3528 (1995)